was chosen for this study. Further, only one link has a V/C ratio value approaching 1, which yielded a substantial random delay contribution. Thus, it is possible that SIGOP-II might not perform better than TRANSYT in a network with more links having V/C ratios near 1 and longer block lengths (or, in fact, if a similar free-flow speed correction factor were applied to TRANSYT).

The results of TRANS and TRANSYT were mixed. TRANS was closer to the field data on a networkwide basis, but in the link-specific sum of squares test, the two models were about even. The reason can be seen from looking at the link-specific results; TRANSYT almost consistently gives a higher value for average speed than is observed in the field, while TRANS often gives a lower value. It is highly probable that the reason why TRANSYT is consistently high is the use of free-flow speed rather than average running speed, which will also be a factor in the TRANS model. In the latter, however, the hit-or-miss Monte Carlo queue-discharge mechanism is equivalent to a negative exponential headway distribution (6). This means that there will be some probability of long headways being generated. These are not observed in field data, unlike UTCS-1 in which the longest headway is 1.8 times the mean headway. This will have the effect of overestimating delay on an intersection approach in which V/C approaches 1.

REFERENCES

1. R. D. Worrall and E. B. Lieberman. Network Flow Simulation for Urban Traffic Control Systems—Phase II. Federal Highway Administration; National Technical Information Service, Springfield, VA, 1973, Vols. 1-5.
2. F. A. Wagner, F. C. Barnes and D. L. Gerlough. Refinement and Testing of Urban Arterial and Network Simulation. U.S. Department of Transportation; National Technical Information Service, Springfield, VA, 1967.
3. D. Robertson. TRANSYT—Users Manual. Federal Highway Administration; National Technical Information Service, Springfield, VA, 1974.
4. E. B. Lieberman and J. L. Woo. SIGOP-II: Program to Calculate Optimal, Cycle-Based Traffic Signal Timing Patterns. Federal Highway Administration; National Technical Information Service, Springfield, VA, 1976.
5. E. Fellinghauser and D. S. Berry. The Effects of Opposing Flow on Left-Turn Reduction Factors at Two-Phase Signalized Intersections. Paper presented at the 53rd Annual Meeting, TRB, 1974.
6. S. M. Ross. Applied Probability Models With Optimization Applications. Holden-Day, San Francisco, CA, 1970.

Publication of this paper sponsored by Committee on Traffic Flow Theory and Characteristics.

Some Properties of Freeway Density as a Continuous-Time, Stochastic Process

A. V. Gafarian, J. Pahl, and T. L. Ward, Department of Industrial and Systems Engineering, University of Southern California, Los Angeles

Density is an important macroscopic parameter of traffic flow. A number of studies have based estimations of the density on a section of roadway on speed and flow measurements at the section entrance and exit. This paper views density as a continuous-time, stochastic process and considers the characteristics of the process itself. The study relied on freeway traffic data previously obtained by sequential aerial photography. Position data were smoothed and interpolated to construct individual trajectories, which were aggregated to obtain continuous vehicle counts in roadway sections of various lengths. Autocorrelation functions and power spectra were calculated for these records. It was found that, for the traffic flow under consideration, correlation time was proportional to freeway section length. The power in the process was concentrated below a cutoff frequency that was inversely related to section length. The implications these results have for sampling real traffic processes are discussed.

Density was recognized as an important parameter early in the study of traffic flow. For example, Greenshields (1) concluded that time mean speed was a linear function of density in vehicles per kilometer. His density, the ratio of flow to the arithmetic average of the speeds of vehicles passing the measurement point, is now known to be a biased estimate of the number of cars on a given roadway section (2, 3).

A number of studies have considered the problem of basing estimations of density on a section of roadway on speed and flow measurements at the section entrance and exit (4, 5, 6, 7, 8, 9). This study views density as a continuous-time, stochastic process and considers some of the characteristics of that process.

The data for this study were originally obtained by taking sequential aerial photographs of a three-lane section of the westbound Long Island Expressway (10). The selected flow sequence had a mean concentration of 9.3 vehicles/lane-km (15 vehicles/lane-mile). This corresponds to the Highway Capacity Manual (11) level of service B. The four test sections, 91, 305, 558, and 853 m (300, 1000, 1830, and 2800 ft) long, are examined in column 1 of the table below (1 m = 3.3 ft).

The sections were nested and centered on the same point in the roadway.

Section No.	Column No. 1 Δx	2 $\hat{n}(\Delta x)$	3 $var(\hat{n})$	4 (τ_e)	5 (f_c)	6 $\frac{1}{2}(f_c)$
1	91	2.57	2.96	3.01	0.190	2.6
2	305	8.48	13.4	7.99	0.0489	10.2
3	558	15.3	25.6	13.3	0.0315	15.9
4	853	23.4	40.1	18.2	0.0256	19.5

where

Δx = the length of the three-lane test section in meters (column 1);

$\hat{n}(\Delta x) = (1/T) \int_0^T \hat{n}(t, \Delta x)dt$, with $\hat{n}(t, \Delta x)$ as the observed number of vehicles in Δx at time t and T = record length (column 2);

$var(\hat{n}) = (1/T) \int_0^T \{[\hat{n}(t, \Delta x)] - [n(\Delta x)]^2 dt\}$ (column 3);

τ_e = the time in seconds at which the autocorrelation function has decayed to 1/e (column 4);

f_c = 90 percent of the power in the process is distributed over frequencies f, $0 \le f \le f_c$, with f and f_c in hertz (column 5); and

$\frac{1}{2}f_c$ = the sampling interval in seconds that yields a Nyquist frequency equal to f_c (column 6).

The original data (10) had previously been reduced to a series of position measurements at 2-s intervals. These measurements were treated as the sum of a systematic part plus a random error. The errors were assumed to be an uncorrelated sequence of random variables with zero mean and known variance.

This is a good approximation to reality. The positions were smoothed, subject to the constraint that the total error was preserved (12), by minimizing the sum of squares of second differences at the measurement points. The smoothed values were then interpolated using a cubic spline procedure (12, 13, 14). The interpolation provided a point estimate of the times each vehicle entered and left the test section.

The smoothing and interpolation were evaluated by a simulation study. Trajectories were constructed to provide a known acceleration spectral density function (12). The parameters of the acceleration spectral density were estimated from the experimental data of Torres (15). Exact section entry and exit times were obtained from these trajectories. The simulated trajectories were sampled at 2-s intervals and corrupted by adding noise, which was known to have a zero mean and 0.19-m^2 (2.0-ft^2) variance. The resulting noisy trajectories were smoothed and interpolated as described above to obtain estimates of the entry and exit times. The magnitude of the differences between the exact and estimated times was found to be generally less than 0.05 s.

DENSITY PROCESS

Continuous time records of the number of cars in three test sections were developed. Figures 1 and 2 show examples of the resulting plots for sections 1 and 3. These records are essentially continuous, in that the number of cars was counted every 0.1 s. This was accomplished by first computing the absolute times of section entry and exit for each vehicle and then simply determining which vehicles were in the test section. This gave the desired point.

The error in estimating boundary-crossing times has been determined to be no larger than 0.05 s. Therefore, the location in time of a jump point in Figure 1 may be off by at most ±0.05 s. Hence, the true function—n(t) equals number of cars in the test section—is equal to the estimated function, $\hat{n}(t)$, plus an error function, e(t). That is, n(t) equals $\hat{n}(t)$ plus e(t). The error function would be a superimposition of three pulse trains—$e_i(t)$—where i = 1, 2, 3, one for each lane. Each pulse of each train would be no wider than 0.05 and would have either a positive or a negative sign. Figure 3 shows, as an

Figure 1. Number of cars versus time for section 1.

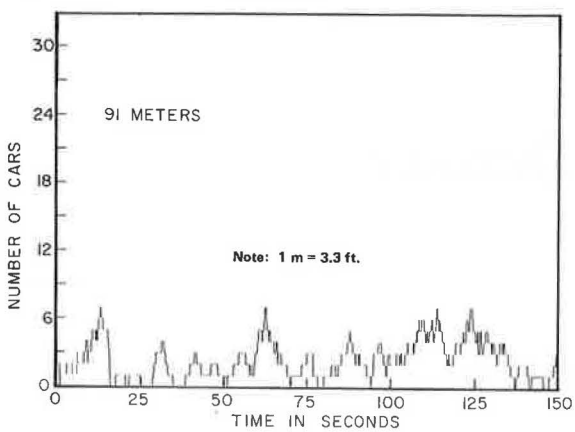

Figure 2. Number of cars versus time for section 3.

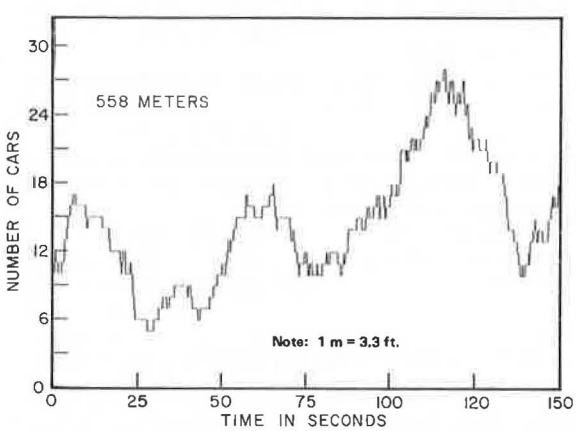

Figure 3. Example of error pulse train superimposed on car-counting process.

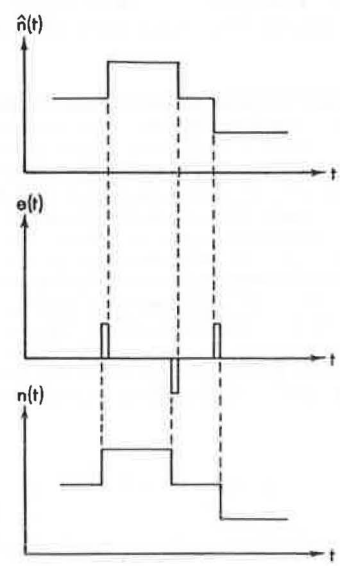

example, a situation in which no pulses occur simultaneously. The first two jumps in $\hat{n}(t)$ occurred 0.05 s later than they should have, while the third jump occurred 0.05 s earlier than it should have.

The average number of jump points per unit time per lane is equal to 2q/3, where q is the freeway flow (or vehicles per unit time for all three lanes). The factor 2 arises because each vehicle causes a jump on entering and leaving the test section. Thus, on the average, the total time per unit time occupied by these pulses is at most (2q) (0.05).

The flow level in this analysis was of the order of 0.75 vehicle/s. Therefore, the error pulses occupy at most 7.5 percent of the time.

To calculate the variance of e(t), we note that it is a zero mean stochastic process, since

$$E[e(t)] = E[e_1(t)] + E[e_2(t)] + E[e_3(t)] \tag{1}$$

and the errors $e_i(t)$, $i = 1, 2, 3$, are ±1 with equal likelihood. Therefore, $E[e_i(t)] = 0$, $i = 1, 2, 3$, and so also $E[e(y)]$. Furthermore, when i does not equal j,

$$E[e_i(t)e_j(t)] = 0 \tag{2}$$

This follows from the fact that the product $e_i(t)e_j(t)$ is also ±1 with equal probability. Thus,

$$\begin{aligned} var[e(t)] &= E[e^2(t)] \\ &= E[e_1^2(t)] + E[e_3^2(t)] \end{aligned} \tag{3}$$

Using the probabilities

$$P[e_i(t) = -1] = (1/2)[(1/3)2q\Delta t] \tag{4}$$

$$P[e_i(t) = 0] = 1 - (1/3)2q\Delta t \tag{5}$$

and

$$P[e_i(t) = 1] = 1/2[(1/3)2q\Delta] \tag{6}$$

where Δt is the pulse width of at most 0.05, it follows that

$$\begin{aligned} E[e_i^2(t)] &= (2)(1)(1/2)[(1/3)2q\Delta t] + 0[1 - (1/3)2q\Delta t] \\ &= (2/3)q\Delta t \end{aligned} \tag{7}$$

For $\Delta t = 0.05$, then

$$var[e(t)] = 2q(0.05) = q/10 \tag{8}$$

and q = 0.75 vehicle/s gives var[e(t)] = 0.075. Column 3 of the table above shows the variance of $\hat{n}$, the observed number of vehicles. Clearly, the variance of the error is small relative to the variance of even the smallest test section.

This error has a negligible effect on the characteristics being studied. For example, consider the autocorrelation function of the stochastic process [n(t)]. This is given by

$$\rho_n(\tau) = (E\{[n(t) - \mu][n(t + \tau) - \mu]\})/\{var[n(t)]\} \tag{9}$$

when

$$E[n(t)] = \mu \tag{10}$$

Replacing n(t) with $[\hat{n}(t)] + [e(t)]$ in Equation 9 and taking expectations gives four terms in the numerator, namely,

1. $E\{[\hat{n}(t) - \mu]\ [n(t + \tau) - \mu]\}$,
2. $E\{[\hat{n}(t) - \mu]\ e(t + \tau)\}$,
3. $E\{[\hat{n}(t + \tau) - \mu]\ e(t)\}$, and
4. $E[e(t)\ e(t + \mu)]$.

But $\hat{n}(t)$ and e(t) are uncorrelated processes, so the middle two expectations are zero. Furthermore, we have

$$E[\hat{n}(t)] = E[\hat{n}(t)] = \mu \tag{11}$$

$$var[\hat{n}(t)] = var[\hat{n}(t)] + 2\ cov[\hat{n}(t), e(t)] \tag{12}$$

But

$$cov[\hat{n}(t), e(t)] = E\{[\hat{n}(t) - \mu]e(t)\} = 0 \tag{13}$$

so that

$$var[n(t)] = var[\hat{n}(t)] \tag{14}$$

Hence, Equation 1 reduces to

$$\rho_n(\tau) = \rho_{\hat{n}}(\tau) + (\{var[e(t)]\}/\{var[\hat{n}(t)]\})\ \rho_e(\tau) \tag{15}$$

where $\rho_n(\tau)$ and $\rho_{\hat{n}}(\tau)$ are the autocorrelation functions of the $\hat{n}(t)$ and e(t) processes respectively. Now $|\rho_e(\tau)| \le 1$ and

$$\{var[e(t)]\}/\{var[\hat{n}(t)]\} << 1 \tag{16}$$

so that

$$\rho_n(\tau) \doteq \rho_{\hat{n}}(\tau) \tag{17}$$

STATISTICAL CHARACTERISTICS OF THE DENSITY PROCESS

The total length of each record used was 720 s, and the sampling interval, as stated earlier, was 0.1 s. With these particular values, it would be possible to distinguish frequency peaks in the spectrum separated by $1/720 = 0.0014$ Hz, and to estimate frequencies as high as $(1/2)/0.1 = 5$ Hz (16).

The autocorrelation and power spectral density estimates follow Blackman and Tukey (16). Program BMD02T of the Biomedical Data Programs (17) was used in these analyses. The autocovariance of the series is first computed by using

$$R(\tau) = [1/(N - p)] \sum_{i=1}^{N-p} (n_i - \bar{n})(n_{i+p} - \bar{n}),\ p = 0, 1, \ldots, m \tag{18}$$

where

$\tau = p\Delta t$,
$m\Delta t$ = maximum lag considered = 180 s,
$N\Delta t$ = total length of the series = 720 s,
$\Delta t = 0.1$ s, and

$$\bar{n} = (1/N) \sum_{i=1}^{N} n_i.$$

Section 4 is $N\Delta t = 178$ s, and the maximum lag considered is $m\Delta t = 44.5$ s, with $\Delta t = 0.1$ s. The number of data points and the number of lags exceeded the limitation of BMD02T. Program modifications were made to accommodate the data. The autocorrelation function is given by

$$r(\tau) = R(\tau)/R(0) \tag{19}$$

Figures 4 and 5 show the autocorrelation functions of sections 1 and 4. Figure 6 shows a plot of the correla-

tion time versus the section length. Correlation time is defined as the time lag at which the autocorrelation function decays to the value 1/e.

An examination of Figures 4 and 5 shows that the autocorrelation functions of the density process can be considered to be initially exponential, followed by an exponentially damped sine curve tail. The correlation time shown in Figure 6 increases almost linearly with section length, which is certainly to be expected. It follows from the fact that, as length increases, a given flow level along with its random fluctuations takes more time to change the number of vehicles in the section from its average.

The estimated one-sided spectrum is calculated in two stages, again using BMD02T (17). First, a truncated, unweighted cosine transform of the data is taken to give a raw estimate of the spectrum:

$$Q(f) = (\Delta/\pi)(r_0 + 2\sum_{k=1}^{m} r_k \cos 2\pi fk) \tag{20}$$

calculated at f = j/4m cycles/s, where j = 0, 1, . . . , 2m. These estimates are then smoothed by using the weights 0.23, 0.54, and 0.23 to give the Hamming estimates

$$P(f) = 0.23Q[f - (1/4m)] + 0.54Q(f) + 0.23Q[f + (1/4m)] \tag{21}$$

at f = j/4m, where j = 1, 2, . . . , 4m - 1. At zero frequency and at the Nyquist frequency

$$P(0) = 0.54Q(0) + 0.46Q(1/4m) \tag{22}$$

$$P(1/2) = 0.54Q(1/2) + 0.46Q[(1/2) - (1/4m)] \tag{23}$$

For a discrete process, the Nyquist frequency $1/(2\Delta t)$ Hz is the highest frequency about which we can get meaningful information from a set of data (18). Plots of the one-sided power spectra are shown in Figures 7 and 8.

An inspection of these figures shows that, as the roadway length increases, the amount of power at the higher frequencies diminishes. A numerical integration was performed to estimate the 90 percent cumulative power

Figure 4. Autocorrelation function for section 1.

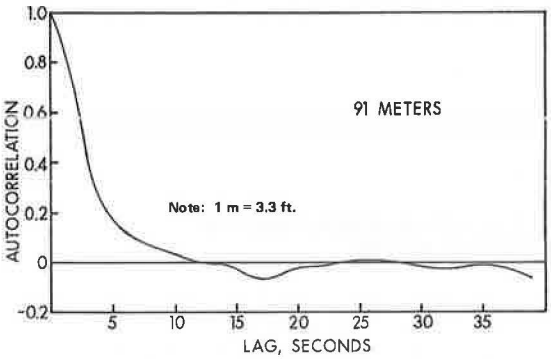

Figure 5. Autocorrelation function for section 4.

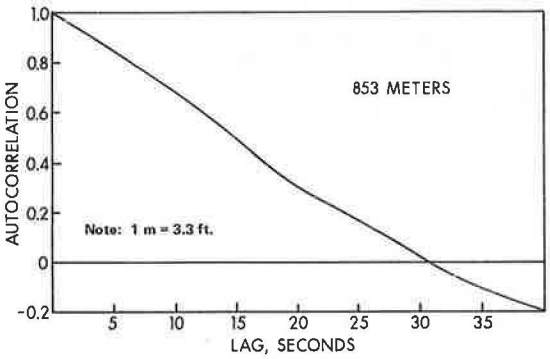

Figure 6. Correlation time versus test-section length.

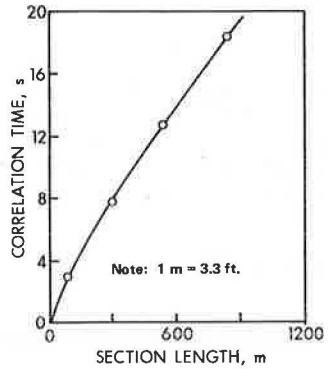

Figure 7. Power spectrum for section 1.

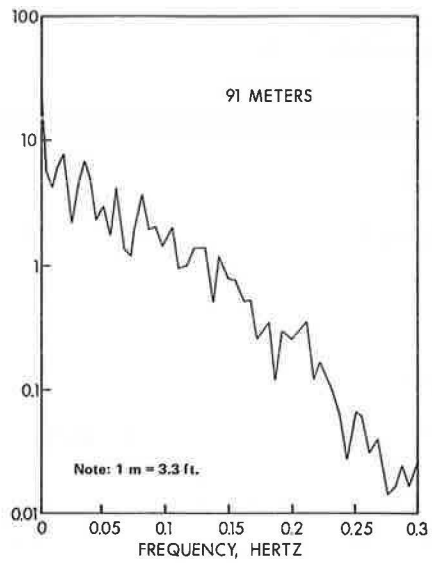

Figure 8. Power spectrum for section 4.

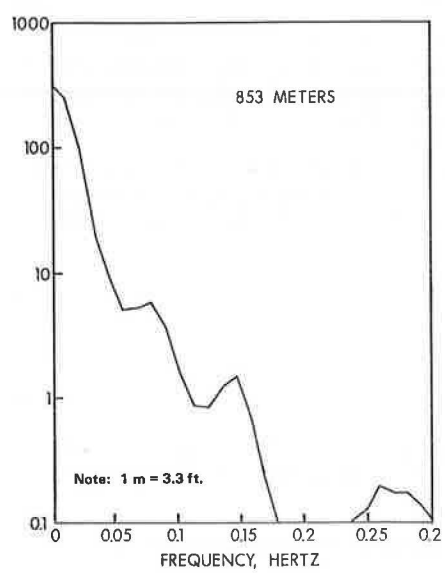

points. These are shown in column 5 of the table given previously.

DISCUSSION

Each of the four series considered in this study is a continuous process sampled every 0.1 s. Thus, the Nyquist frequency is 5.0 Hz. In sampling a continuous time series, an important question is how to choose the sampling interval. It is clear that sampling leads to some loss of information and that this loss gets worse as the sampling interval Δt increases. If Δt is too large, "aliasing" may occur. This is the phenomenon in which variation in the continuous process at frequencies above the Nyquist frequency will be "folded back" and will produce an effect at lower frequencies. If the continuous series contains no variation at frequencies above the Nyquist frequency, then the spectra of the continuous and sampled processes are the same. In this case, no information is lost by sampling.

From a practical point of view, aliasing will cause trouble unless the Δt chosen is so small that the spectrum of the continuous process is essentially zero for frequencies larger than $\frac{1}{2}\Delta t$. If, for a given Δt, the spectrum estimate approaches zero near and above the Nyquist frequency, then the choice of Δt is sufficiently small. Clearly, in each of the cases shown in the table, this obtains for frequencies larger than 5 Hz.

In another study (19), three of the cases reported in our table, namely, the 91-, 305-, and 558-m (300-, 1000-, and 1830-ft) records were sampled at intervals of 2, 5, and 5 s respectively.

The time-series analytical techniques of Box and Jenkins (20) were used to identify the structure of autoregressive models for each of the three. Model parameters were then estimated and statistically tested. It was found that reasonable forecasts of the density could be made for lead times comparable to the correlation times (column 4 of the table).

REFERENCES

1. B. D. Greenshields. A Study of Traffic Capacity. Proc., HRB, Vol. 14, Pt. I, 1935, pp. 448-477.
2. M. J. Lighthill and G. B. Whitman. On Kinematic Waves II. A Theory of Traffic Flow on Long Crowded Roads. Proc., Royal Society of London, Series A, Vol. 229, No. 1178, May 10, 1955, pp. 317-345.
3. L. Brieman. Space-Time Relationships in One-Way Traffic Flow. Transportation Research, Vol. 3, No. 3, Sept. 1969, pp. 365-376.
4. D. C. Gazis and R. S. Foote. Surveillance and Control of Tunnel Traffic by an On-Line Digital Computer. Transportation Science, Vol. 3, No. 3, Aug. 1969, pp. 255-275.
5. D. C. Gazis. On-Line Estimation of Traffic Densities From Time-Series of Flow and Speed Data. Transportation Science, Vol. 5, No. 3, Aug. 1971, pp. 283-301.
6. C. H. Knapp. Traffic Density for Single and Multilane Traffic. Transportation Science, Vol. 7, No. 1, Feb. 1973, pp. 75-84.
7. N. E. Nahi and A. N. Trivedi. Recursive Estimation of Traffic Variables: Section Density and Average Speed. Transportation Science, Vol. 7, No. 3, Aug. 1973, pp. 269-286.
8. D. C. Gazis and M. W. Szeto. Design of Density-Measuring Systems for Roadways. TRB, Transportation Research Record 495, 1974, pp. 44-52.
9. M. F. Chang and D. C. Gazis. Traffic Density Estimation With Consideration of Lane-Changing. Transportation Science, Vol. 9, No. 4, Nov. 1975, pp. 308-320.
10. P. K. Munjal and Y. S. Hsu. Characteristics of Freeway Traffic. Analytical Models of Multi-Lane Traffic Flow, Vol. 1, Federal Highway Administration, contract no. FH-11-7628, 1972.
11. Highway Capacity Manual. HRB, Special Rept. 87, 1965.
12. R. Agahi, A. V. Gafarian, P. Jaffer, L. T. Nguyen, and J. Pahl. Characteristics of Multilane Traffic Flow From Aerial Data. Department of Industrial and Systems Engineering, Univ. of Southern California, Los Angeles, Technical Rept. 76-2, Oct. 1976.
13. J. J. Ahlberg, E. N. Nilson, and J. L. Walsh. The Theory of Splines and Their Applications. Academic Press, New York, 1967.
14. J. J. Schoenberg, ed. Approximation With Special Emphasis on Spline Functions. Academic Press, New York, 1969.
15. J. F. Torres. Acceleration Noise, Power Spectra, and Other Statistics Derived From Instrumented Vehicle Measurements Under Freeway Driving Conditions. System Development Corporation, Santa Monica, CA, TM-3858/025/00, Sept. 30, 1969.
16. R. E. Blackman and J. W. Tukey. The Measurement of Power Spectra. Dover, New York, 1958.
17. W. J. Dixon, ed. BMD Biomedical Computer Programs, Univ. of California Press, Los Angeles, 1970.
18. G. W. Jenkins and D. G. Watt. Spectral Analysis and Its Applications. Holden-Day, San Francisco, 1968.
19. A. V. Gafarian, J. Pahl, and T. L. Ward. Discrete Time Series Models of a Freeway Density Process. Proc., 7th International Symposium on Transportation and Traffic Theory. Institute of Systems Science Research, Kyoto, 1977, pp. 387-411.
20. G. E. P. Box and G. M. Jenkins. Time Series Analysis Forecasting and Control, Holden-Day, San Francisco, rev. ed., 1976.

Publication of this paper sponsored by Committee on Traffic Flow Theory and Characteristics.